dies for Two-Dimensional Wedges and Curved Surfaces at Mach Numbers of 4.8 to 6.2," NASA TN D-1014, Feb. 1962.

[7]Todisco, A., and Reeves, B. L., "Turbulent Boundary-Layer Separation and Reattachment at Supersonic and Hypersonic Speeds," *Proceedings of Viscous Interaction Phenomena in Supersonic and Hypersonic Flow,* USAF Symposium, Aerospace Research Labs., Dayton, OH, May 1969, p. 139.

[8]Disimile, P. J., and Scaggs, N. E., "The Effect of Separation on Turbulent Boundary Layer Characteristics Over a Smooth Surface at Mach 6.0," AIAA Paper 90-3028, Portland, OR, Aug. 1990.

[9]Roshko, A., and Thomke, G. J., "Flare-Induced Interaction Lengths in Supersonic, Turbulent Boundary Layers," *AIAA Journal,* Vol. 14, No. 7, 1976, pp. 873-879.

[10]Disimile, P. J., and Scaggs, N. E., "High Reynolds Number Wedge-Induced Separation Lengths at Mach 6," *AIAA Journal,* Vol. 27, No. 12, 1989, pp. 1827-1828.

[11]Selig, M. S., Andreopoulos, J., Muck, K. C., Dussauge, J. P., and Smits, A. J., "Turbulence Structure in a Shock Wave/Turbulent Boundary-Layer Interaction," *AIAA Journal,* Vol. 27, No. 7, 1989, pp. 862-869.

Surface Flow Patterns on an Ogive-Cylinder at Incidence

David Degani,* Murray Tobak,† and G. G. Zilliac‡
NASA Ames Research Center,
Moffett Field, California 94035

I. Introduction

It is well known that the flow about a body of revolution becomes asymmetric with respect to the angle of attack plane at a sufficiently high angle of attack (cf. Refs. 1-7). This asymmetry may be altered by changing the roll angle position of the nose of the body[5,6] or by placing a small asymmetrically disposed disturbance near the apex.[5,7] With further increase in incidence, the steady asymmetric flow becomes unsteady, and as the angle of attack tends toward 90 deg, the flow pattern approaches that of a circular cylinder in crossflow.

Degani and Zilliac[4] have shown experimentally that in addition to the low-frequency von Kármán vortex shedding from the cylinder portion of an ogive-cylinder body at very high incidence, and a high-frequency unsteadiness resulting from a traveling-wave instability of the shear layer, the flow exhibited a midrange frequency unsteadiness as well (with Strouhal number about twice that associated with von Kármán vortex shedding). Although its source has not been identified, this unsteadiness was found to be limited to angles of attack between 50 and 65 deg. The maximum signal level of fluctuations (using a hot-wire anemometer) was found in a volume of about 4D long × 2D high × 2D wide centered above the ogive-cylinder junction. It was suggested in Ref. 4 that this midrange frequency was the result of vortex interaction.

Zillac et al.[5] and other researchers[3,6] have found experimentally that in the range of angles of attack between 50 and 65 deg the flowfield behaves differently than it does at angles of attack both above and below this range when a small change is enforced on the flowfield. When the nose roll angle changed smoothly, the flow above the body changed between two stable positions only. A rational explanation for this behavior of the flowfield was suggested by Tobak et al.[8] with the support of preliminary, unpublished results of the present paper. According to these results, in the range of angles of attack between 50 and 65 deg, foci may exist in the forebody surface flow pattern on the line of primary separation on each side of the body.

It seems clear that the occurrence of a particular regime of flow unsteadiness at angles of attack between 50 and 65 deg and the bistable nature of the flow within this same angle-of-attack range must be linked to the coincident appearance of foci in the surface flow patterns. In view of the potential importance of the phenomenon in completing our understanding of the flow over bodies at incidence, we consider it worthwhile to document the event more fully. This paper contains a complete set of photographs of the surface flow patterns, obtained for angles of attack between 30 and 85 deg, flow conditions at a Reynolds number of 2.6×10^4.

II. Experimental Approach and Results

Measurements were performed in a 38 × 38 cm, low-turbulence wind tunnel at velocities ranging from 12 to 24 m/s. The maximum freestream turbulence level of this facility, as measured by a hot-wire anemometer, is 0.15%. The quality of wind-tunnel flow has been documented more fully in an internal NASA memorandum, available on request to the authors. Although we recognize that freestream turbulence properties might have influenced the shape and extent of the phenomenon to be reported here, we consider it highly unlikely that they could have caused it to appear. Likewise, we consider that other sources of flow unsteadiness and gravitational force effects, which are always present to an undetermined extent in flow-visualization studies, could not have been the cause of the phenomenon to be reported here.

The model configuration consisted of an $L/D = 3.5$ tangent ogive with an $L/D = 12.5$ cylindrical afterbody. The overall length of the model was 35 cm and the diameter of the cylindrical afterbody portion of the model was 2.16 cm. The model was mounted rigidly on a sting support. No boundary-layer trips were used to stabilize the vortex positions or to cause boundary-layer transition. Judging by the position of the lines of separation on the model, we consider the boundary layer to have been laminar. Maximum wind-tunnel model blockage, based on the projected frontal area of the model, was < 5.0% of the cross-sectional area of the test section at 90 deg angle of attack.

Owing to the relatively low freestream velocity and also the inclination of the model, it was necessary to develop a surface flow visualization medium that was less viscous than the standard oil-titanium oxide mixture. After extensive experimentation, a mixture by volume of approximately 5.0% oil-based black paint, 40.0% paint thinner, and 55.0% kerosene was adopted. It was found that, with brush application, a smooth, thin coat could be applied that would flow readily and dry within a few minutes at the freestream velocities of the test.

Experiments were made at a Reynolds number of 2.6×10^4 with angles of attack ranging from 35 to 85 deg. Figures 1 present photographs of oil flow patterns obtained under the previously mentioned conditions. For each angle of attack, three views are shown: left side, top (leeward) side, and right side. Because the paint was highly thinned to allow better capturing of the separation and reattachment lines, the surface pressure gradient was sufficient to blow away the oil on the windward side. Therefore, this view is omitted in Figs. 1. After the completion of each run, the model was taken out of the wind tunnel and the photographs were taken. At each angle of attack, several experiments were carried out resulting in similar surface flow patterns. In all cases, the reference roll angle was kept unchanged. The circumferential angle of the separation line is about 90 deg from the windward ray for all

Received Aug. 23, 1990; revision received Oct. 26, 1990; accepted for publication Dec. 6, 1990.

*Associate Professor, on leave from Technion—Israel Institute of Technology, Faculty of Mechanical Engineering, Haifa, Israel. Associate Fellow AIAA.

†Staff Scientist. Associate Fellow AIAA.

‡Research Scientist.

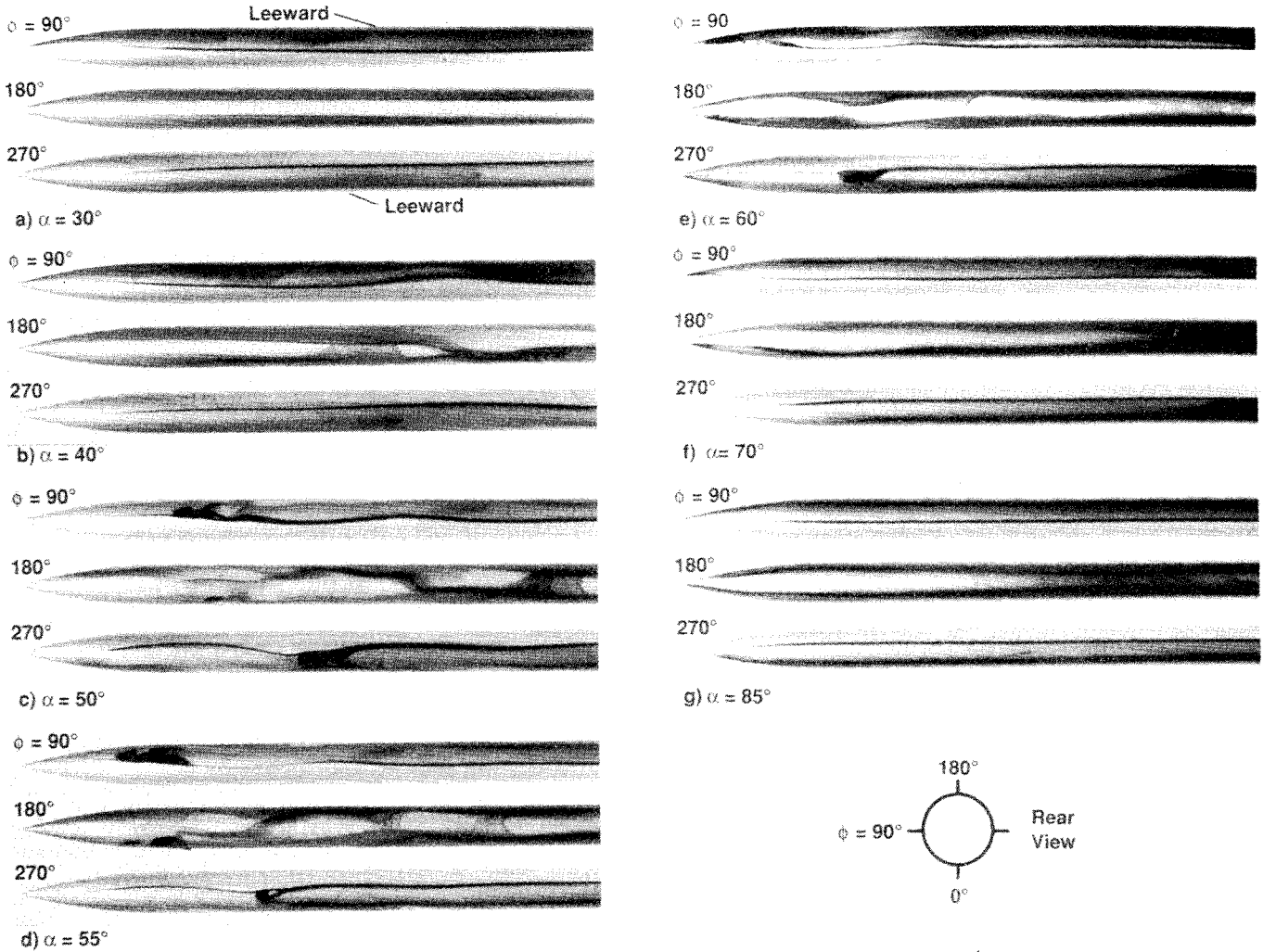

Fig. 1 Photographs of oil flow patterns on an ogive cylinder: $Re_D = 2.6 \times 10^4$.

angles of attack, which indicates that the flow separation is laminar. For angles of attack of 30 and 40 deg, the primary separation line is continuous and almost straight except for some waviness in the area near the aft of the body (Fig. 1b, $\phi = 90$ deg) where the primary vortices are asymmetric, crossing the leeward plane of symmetry at angle of attack of 40 deg (Fig. 1b, $\phi = 180$ deg). For angles of attack of 50, 55, and 60 deg, foci of separation are present on the lines of separation. Because of the bistable state of the flow in this angle-of-attack range, a change in the roll angle of the nose may reveal the image picture. Figures 2 show the details of the foci, and the location of the foci relative to the separation line can be seen more clearly. While performing the experiments, we have noticed that the oil was attracted to the foci and created thick bubbles. As the angle of attack increases, the foci move forward and they disappear as the angle of attack approaches 70 deg. At 70 and 85 deg, although the flow is highly unsteady and instantaneously asymmetric, the mean flow near the surface is symmetric, the effect of the tip vortices is negligible, and, therefore, the separation lines are symmetric and straight.

III. Discussion and Conclusions

It was suggested[8] that the foci act as the anchor points that allow the stream surfaces containing the castoff vortical structures from the forebody to roll up in the wake and form the forebody's trailing vortex system. Figure 3 shows schematically how a focus might carry out this role on an ogive cylinder. By allowing the stream surfaces containing the pair of castoff vortical structures to roll up in the wake, the foci enable the formation of a trailing vortex system that is virtually independent of the details of the nose geometry. Although not proved, it seems evident that the appearance of these foci is closely associated with the bistable nature (cf. Refs. 3, 5, and 6) of the flowfield. Before the foci appear, flowfield properties vary continuously with variations of the roll angle position of the nose. After the foci appear, the flowfield properties change and become bistable with virtually a square-wave variation with variations of the nose roll angle. As the angle of attack increases above 65 deg, the effect of the foci decreases and the unsteady nature of the flowfield becomes dominant.

The discovery of the foci, at least for a limited range of angles of attack and Reynolds numbers, brings up several important questions:

1) Is the appearance of foci in the surface flow topology of an ogive cylinder an expression of the same mechanism that underlies their known appearance on blunt-nosed bodies such as the hemisphere cylinder?

2) Does the appearance of foci signal a fundamental change in the instability mechanisms that are in play before the change in surface flow topology?

3) Does the use of the concept of crossflow separation (i.e., separation in the component of flow lying in a crossflow plane, cf. Ref 9) for sharp-tip bodies become invalid with the appearance of foci in the surface flow topology? This bears on the question of an appropriate turbulence modeling for slender bodies at incidence. Although the results presented here did not change much with Reynolds number in the range tested (1.7×10^4–3.5×10^4), it is not known whether this phenomenon exists at much higher Reynolds numbers (i.e.,

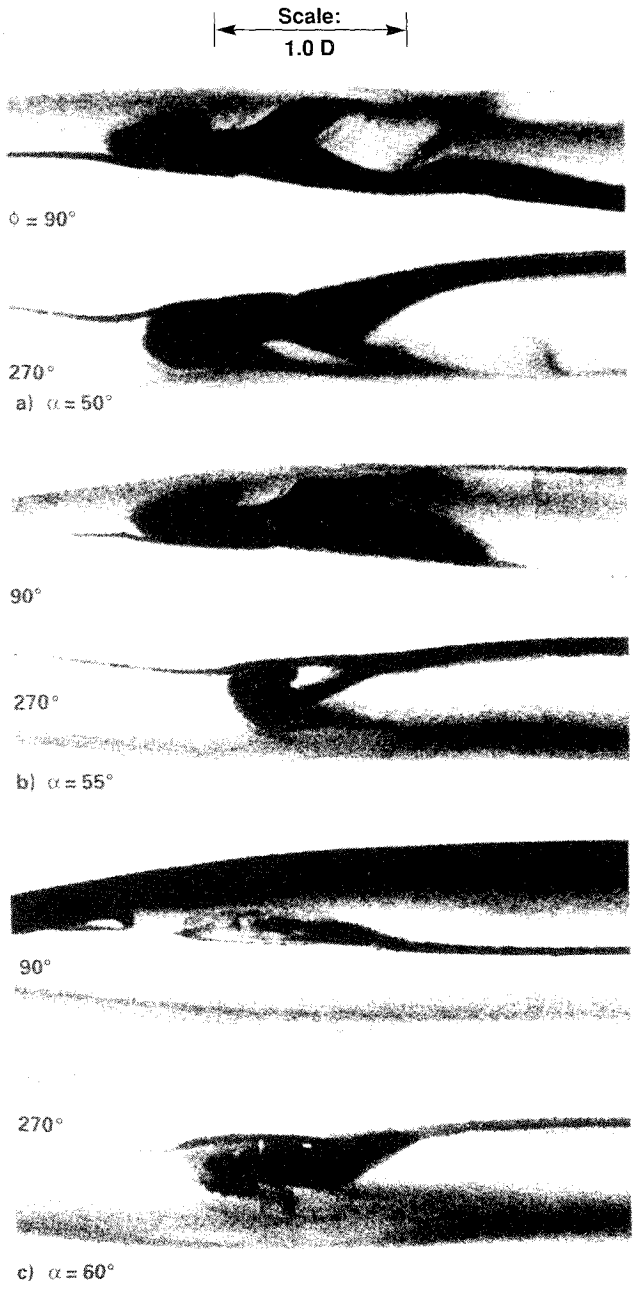

Fig. 2 Details of foci on an ogive cylinder: $Re_D = 2.6 \times 10^4$.

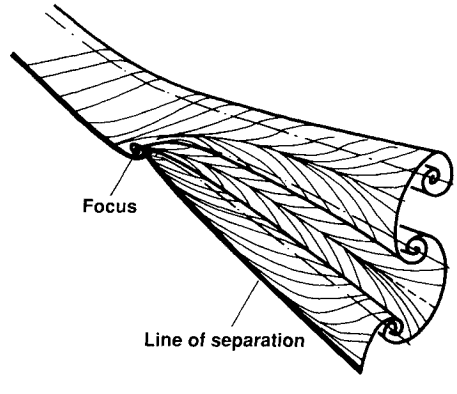

Fig. 3 Conjectured mechanism for formation of trailing-vortex system on an ogive cylinder.

under turbulent flow conditions). If it does, this will be evidence that the crossflow separation on a slender body at incidence has become a regular three-dimensional separation, which will pose a more difficult problem for computational simulation.

References

[1]Hunt, B. L., "Asymmetric Vortex Wakes on Slender Bodies," AIAA Paper 82-1336, Aug. 1982.

[2]Ericsson, L. E., and Reding, J. P., "Aerodynamic Effects of Asymmetric Vortex Shedding from Slender Bodies," AIAA Paper 85-1797, Aug. 1985.

[3]Lamont, P. J., "Pressures Around an Inclined Ogive-Cylinder with Laminar, Transitional, or Turbulent Separation," *AIAA Journal,* Vol. 20, No. 11, 1982, pp. 1492–1499.

[4]Degani, D., and Zilliac, G. G., "An Experimental Study of the Nonsteady Asymmetric Flow Around an Ogive-Cylinder at Incidence," *AIAA Journal,* Vol. 28, No. 4, 1990, pp. 642–649.

[5]Zilliac, G. G., Degani, D., and Tobak, M., "Asymmetric Vortices on a Slender Body of Revolution," *AIAA Journal,* Vol. 29, No. 5, pp. 667–675.

[6]Dexter, P. C., and Hunt, B. L., "The Effects of Roll Angle on the Flow Over a Slender Body of Revolution at High Angle of Attack," AIAA Paper 81-0358, Jan. 1981.

[7]Moskovitz, C. A., Hall, R. M., and DeJarnette, F. R., "Effects of Nose Bluntness, Roughness and Surface Perturbations on the Asymmetric Flow Past Slender Bodies at Large Angles of Attack," AIAA Paper 88-2236, Aug. 1989.

[8]Tobak, M., Degani, D., and Zilliac, G. G., "Analytical Study of the Origin and Behavior of Asymmetric Vortices," NASA TM-102796, April 1990.

[9]Chapman, G. T., "Topological Classification of Flow Separation on Three-Dimensional Bodies," AIAA Paper 86-0485, Jan. 1986.

Interaction of a Planar Shock Wave with a Double-Wedge-Like Structure

G. Ben-Dor*
Ben-Gurion University of the Negev,
Beer Sheva, Israel

Introduction

THE reflection of a planar shock wave over a double wedge is a relatively new topic of research initiated a few years ago by Ben-Dor et al.[1] In their study they established that, for a given incident shock wave Mach number M_i, there are seven different domains of reflection processes in the (θ_w^1, θ_w^2) plane, where θ_w^1 and θ_w^2 are the angles of the first and second surfaces of the double wedge. The inclination of the second surface with respect to the first one is $\Delta\theta_w = \theta_w^2 - \theta_w^1$. Schematical drawings of a concave and convex double wedge are shown at the bottom of Fig. 1.

The seven domains of the different types of the reflection process of a planar shock wave over a double wedge in the (θ_w^1, θ_w^2) plane are shown in Fig. 1. The line $\Delta\theta_w = 0$ divides the (θ_w^1, θ_w^2) plane into the domains of a concave double wedge $(\Delta\theta_w > 0)$ and a convex double wedge $(\Delta\theta_w < 0)$. The line $\theta_w^1 = \theta_w^{tr}|_{M_i}$ (where $\theta_w^{tr}|_{M_i}$ is the RR↔MR transition wedge angle appropriate to the incident shock wave Mach number M_i) determines the initial type of reflection over the first surface. If $\theta_w^1 < \theta_w^{tr}|_{M_i}$, then the shock wave reflects over the first surface as a Mach reflection (MR), and if $\theta_w^1 > \theta_w^{tr}|_{M_i}$, then the reflection of the shock wave over the first surface is regular (RR). The line $\theta_w^2 = \theta_w^{tr}|_{M_i}$ determines the type of the reflection that is

Received July 31, 1990; revision received Oct. 10, 1990; accepted for publication Oct. 10, 1990.

*Department of Mechanical Engineering, Pearlstone Center for Aeronautical Engineering Studies.